

TEM, XANES AND NANOSIMS CHARACTERIZATION OF CARBONACEOUS PHASES FROM INDIVIDUAL STARDUST AND IDP PARTICLES. G. Matrajt, *Department of Astronomy, University of Washington, Seattle WA, 98195 (matrajt@astro.washington.edu)*, S. Messenger, *Johnson Space Center 2101 NASA Pkwy Houston TX, 77058*, M. Ito, *Johnson Space Center 2101 NASA Pkwy Houston TX, 77058*, S. Wirick, *Department of Physics and Astronomy, State University of New York at Stony Brook, Stony Brook, New York 117943800*, G. Flynn, *Department of Physics, SUNY-Plattsburgh, 101 Broad Street, Plattsburgh, New York 12901*, D. Joswiak, *Department of Astronomy, University of Washington, Seattle WA, 98195*, D. Brownlee, *Department of Astronomy, University of Washington, Seattle WA, 98195*.

Introduction: We present results of a coordinated investigation of the carbonaceous phases of four Stardust (SD) particles and three interplanetary particles (IDPs) using TEM, XANES and NanoSIMS. The SD samples are Coki (a fragment in track # 141), Bidi (the terminal particle of track # 130), and Tule and Isis which are debris along the walls of tracks # 80 and # 41. Coki is a 1.1 mm long bulbous-type track that contains pentlandite, augite, olivine, anorthite, fassaite and diopside with traces of spinel and V-Nb inclusions [1]. Bidi is a 1.3 mm long carrot-type track composed of olivine, augite and anorthite [2]. The IDPs were named Plin (W7154-1I), Pupi (U2-20-GCA cluster particle) and Chocha (W7154B-6J). All the IDPs had chondritic elemental abundances based on EDX spectra. Pupi is a porous particle, Plin is a combination of porous and smooth and Chocha is a smooth particle. Here we investigated C-rich areas in both groups of particles by TEM, followed by XANES and NanoSIMS analyses. Our goal was to establish whether each morphological type of carbon exhibited distinct XANES spectra and/or isotopic compositions.

Analytical Methods: The tracks with the particles, received inside aerogel keystones, were processed using the "acrylic embedding" technique developed at the University of Washington [3]. The IDPs were embedded in acrylic after having the silicone oil removed with hexane. Contiguous ultramicrotomed sections of various thicknesses (70 to 95 nm) were placed over Au or Cu TEM grids. The acrylic was removed using condensed chloroform vapors. Then, the grids were analyzed with a 200 kV Tecnai F20 FEG STEM equipped with an energy dispersive X-ray (EDX) detector and a Gatan Imaging Filter (GIF) detector, used to locate and map the carbon with Electron Energy Loss Spectroscopy (EELS) and an orius CCD camera, used to obtain high resolution images of the carbonaceous areas. Samples where carbon was present were then analyzed by XANES and NanoSIMS. XANES data was obtained at the National Synchrotron Light Source (NSLS) at Brookhaven National Laboratory, using a X-ray microscope. Samples were analyzed at the C and O K shell edges. The beamline was focused to 25 microns resulting in an energy resolution for the C K edge of 0.05 eV, and for the O K shell edge of 0.2 eV. CO₂ and O₂ were used to calibrate the spherical grating monochromator position. Isotopic data were obtained with the Johnson Space Center NanoSIMS 50L ion microprobe. Images of ¹²C⁻, ¹³C⁻, ¹²C¹⁴N⁻, ¹²C¹⁵N⁻, ¹⁶O⁻, ¹⁷O⁻, and ¹⁸O⁻ were acquired simultaneously in multidetector with electron multipliers. The isotopic images were acquired by rastering a 16 keV, 1 pA Cs⁺ ion beam focused to 100 nm. Nearby grains of 1-hydroxyl benzotriazole hydrate,

USGS24 graphite, and San Carlos olivine were measured as N, C, and O isotopic standards, respectively. The amorphous C film substrate served as a secondary isotopic standard, providing an isotopic reference during the sample analysis. The surrounding aerogel and a sample of the acrylic used as the embedding medium were also measured and their isotopic values were found to be normal within 1 sigma errors.

TEM Results: The TEM-EELS studies showed that all the particles analyzed contain carbon. Carbon was imaged using a high resolution camera at different magnifications and this procedure revealed that carbon is present in four different types of morphologies (Fig. 1) that we have named: globular (filled or hollow round-shaped globules); vesicular (lacey-shaped vesicles); smooth (shapeless chunks with a smooth surface); and solid with bubbles (elongated shapeless regions that have solid or smooth surfaces with small voids embedded). All the particles studied have at least two of these morphologies. Generally, SD particles have very discreet carbonaceous areas, ranging in size from 100-500 nm whose morphologies are usually vesicular, globular and/or smooth. IDPs are much more rich in carbon than SD particles, with several carbonaceous areas within a single particle, ranging in sizes from 100 nm to several microns, making 10-95 % of the particle's microtomed section. All four morphologies have been found in IDPs, sometimes all of them within the same particle. Particle Chocha, in particular, is very interesting given that it is 95 % carbonaceous (Fig. 2) and all the four morphologies are found in discreet areas that do not overlap with each other but show very clear boundaries.

NanoSIMS Results: For all the particles studied, the $\delta^{13}\text{C}$ values are normal. IDPs: Particle Plin has normal $\delta^{15}\text{N}$ values. Particles Pupi and Chocha have a variety of values for the different morphologies summarized in Table 1. Errors are all 1 σ . SD: Particles Coki and Tule have normal $\delta^{15}\text{N}$ values. Particle Bidi has a discreet carbonaceous area composed of a globule surrounded by vesicular carbon whose $\delta^{15}\text{N}$ value is 252 ± 92 ‰. Isis has not yet been measured.

XANES Results: All four morphologies have a peak at 285 eV, corresponding to a C=C bonding. The narrowness of the peaks varies in the different morphologies suggesting that the material is slightly different, but this could also be due to differences in the thickness of the material throughout the section. The spectra of the globular and vesicular morphologies have also a small peak at 288.5 eV corresponding to a C=O bonding and which is absent in the spectra of the other morphologies. This shows that the carbonaceous materials with different morphologies differ also in chemical composition. A comparison of the XANES spectra obtained from each type of

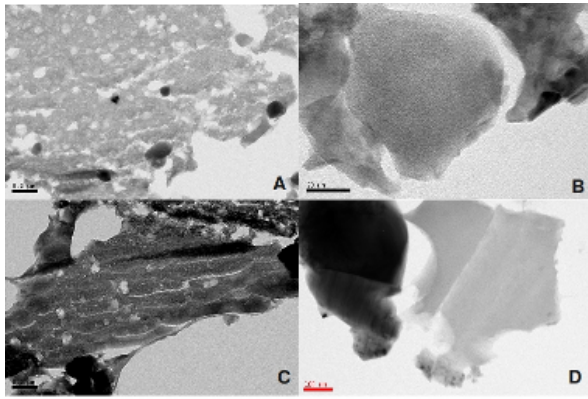


Figure 1: A) Vesicular. The embedded dark grains are sulfides. B) Globular. The example is a filled globule, but hollow globules have also been observed. C) Solid with bubbles. The “bubbles” are the round voids embedded in the carbonaceous material. D) Smooth.

Particle	Morphology	$\delta^{15}\text{N}$ (‰) $\pm 1\sigma$
Chocha	Bulk	273 \pm 7
	Solid with bubbles	286 \pm 18
	Vesicular	241 \pm 9
	Smooth	314 \pm 32
	Globular	too small to be measured
	Hotspot	970 \pm 160
Pupi	Bulk	not determined
	Globular	1003 \pm 124
	Solid with bubbles	424 \pm 50
	Vesicular	290 \pm 53
Coki	vesicular	-5.9 \pm 3.8
	solid	68.9 \pm 61.5
Bidi	globular	252 \pm 92
	vesicular	-53 \pm 107
Tule	smooth	180 \pm 140
Isis	unknown	not available

Table 1. Isotopic values for SD and IDP samples.

carbon morphology is shown in Fig. 3.

Conclusions: Although the carbon abundance is lower in SD particles, both SD and IDPs present the four morphologies studied here. The carbon morphologies have various isotopic and chemical compositions, with $\delta^{15}\text{N}$ isotopic values ranging from “normal (or terrestrial)” to as high as 1000 ‰. H and N isotopic anomalies have already been observed in primitive meteorites, IDPs, and Stardust samples [4-6], where the organic globule morphology is commonly associated with some of the highest H and N anomalies [7]. It is believed that these isotopic anomalies probably originated from low temperature chemical fractionation in the outer solar system or cold molecular cloud [5], suggesting that the carbonaceous grains in our particles formed in different regions of the Solar System (or beyond) before they aggregated to form the parent body.

References: [1] Ishii et al (2009) *LPS XL*, Abstract # 2288. [2] Joswiak et al (2010) *LPS XLI*, this conference. [3] Matrajt and Brownlee (2006) *M&PS*, **41**, 1715-1720. [4] Busemann H. et al. (2006), *Science* **312**, 727. [5] Messenger S. (2000) *Nature* **404**, 968. [6] Matrajt G. et al (2008) *M&PS*, **43**,

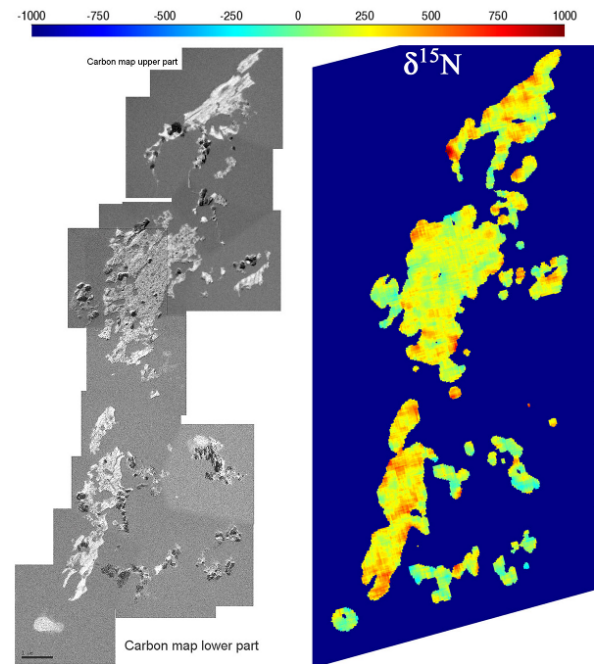


Figure 2: Carbon (left) and $\delta^{15}\text{N}$ (right) maps of particle Chocha. The white areas in the C-map are carbonaceous.

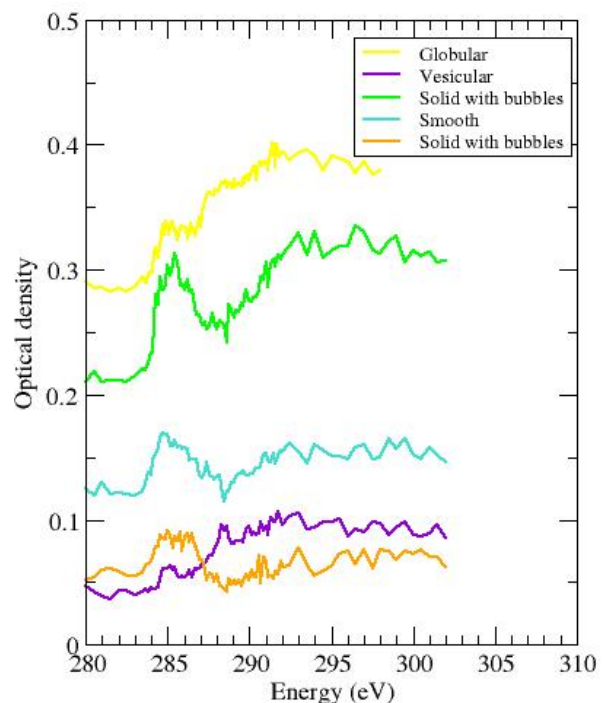


Figure 3: Representative XANES spectra of the different carbon morphologies.

315-334. [7] Messenger S. et al (2008) *LPS XXXIX*, Abstract # 2391.